Colloid Polym Sci (2008) 286:1361–1368
DOI 10.1007/s00396-008-1904-0

ORIGINAL CONTRIBUTION

Aerosol assisted synthesis of silica/phenolic resin composite mesoporous hollow spheres

Xianglin Yu · Shujiang Ding · Zhaokai Meng · Jiguang Liu · Xiaozhong Qu · Yunfeng Lu · Zhenzhong Yang

Received: 29 April 2008 / Revised: 7 June 2008 / Accepted: 16 June 2008 / Published online: 31 July 2008

Abstract Hollow spheres of phenolic resin/silica composite are synthesized by macroscopic phase separation of a sorbitan monooleate surfactant Span 80 during aerosol-assisted spraying. The cavity can be evolved from multiple compartments to single hollow cavity with the increase of Span 80 content. The composite shell becomes mesoporous due to the release of small molecules after thermal treatment above 350 °C. After further thermal treatment at a higher temperature for example 900 °C in nitrogen or 1,450 °C in argon, the carbon/silica composite hollow spheres or crystalline silicon carbide hollow spheres are derived, respectively. Compared to the pure phenolic resin-based carbon spheres, thermal stability of the carbon-based composite spheres in air is essentially improved by the introduction of inorganic component silica. The carbon-based composite hollow spheres combine both performances of easy mass transportation through macropores and high specific surface area of mesopores, which will be promising to support catalysts for fuel cells.

Keywords Hollow spheres · Mesoporous · Carbon · Composite · Template

Electronic supplementary material The online version of this article (doi:10.1007/s00396-008-1904-0) contains supplementary material, which is available to authorized users.

X. Yu · S. Ding · Z. Meng · J. Liu (✉) · X. Qu · Z. Yang (✉)
State Key Laboratory of Polymer Physics and Chemistry,
Institute of Chemistry, Chinese Academy of Sciences,
Beijing 100190, People's Republic of China
e-mail: jiguangl@iccas.ac.cn
e-mail: yangzz@iccas.ac.cn

Y. Lu (✉)
Chemical and Biomolecular Engineering Department,
University of California at Los Angeles,
Los Angeles, CA 90095, USA
e-mail: luucla@ucla.edu

Introduction

Mesoporous hollow silica spheres with both easy mass transportation through macropores and high surface area of mesopores performances integrated together [1–5] have been widely investigated due to their potential applications in drug delivery [6–8], catalysis [9], absorption/separation [10], sensing, and optical active materials [11]. They are mainly synthesized by formation of a mesostructured silica coating using amphiphilic molecule templates onto a colloid template followed by a sequent removal of both templates [9, 12, 13]. It is important to introduce carbon to the mesoporous silica materials to bring new properties such as electron conductivity. Organosilanes are commonly used as inorganic precursors to derive carbon/silica composites [14–16]. Alternatively, infiltration of carbon sources into the mesoporous silica has been extensively employed since this procedure is simple and general. For example, carbon/silica composites have been synthesized by polymerization of a monomer such as acrylonitrile inside silica mesopores followed by further carbonization [17]. Natural materials such as sucrose have also been used to introduce carbon within silica mesopores [18, 19]. However, the mesopores are usually jammed by carbon, which greatly restricts their practical applications. Recently, Liu et al. have reported an approach to prepare the mesoporous silica/phenolic resin composite film through a multicomponent self-assembly process [20, 21]. In principle, the mesopores is guaranteed to be open. Based on this multicomponent self-assembly, we have previously processed the phenolic resin/silica composite into mesoporous spheres using aerosol-assisted method [22, 23]. However, no hollow cavity is formed. It is required to develop a general method to prepare the mesoporous hollow spheres.

It is well known that some polymers can experience macroscopic phase separation, which can be used to obtain macroporous silica [24]. Hollow silica spheres are, thus, synthesized by aerosol-assisted spraying using the phase separation of polymers [25]. In this article, based on the macroscopic phase separation of Span 80, we have prepared the phenolic resin/silica composite hollow spheres using the aerosol-assisted method. It is crucial to use such a surfactant Span 80, which can experience a macroscopic phase separation during solvent evaporation giving some domains. These domains can be used as templates for multiple or single compartments of hollow spheres. The size of the hollow cavity can be controlled by adjusting Span 80 content. The composite shell can be further transformed into carbon/silica network with the morphology preserved, whilst the shell becomes mesoporous arisen from the release of small molecules during thermal treatment at a high temperature. Furthermore, crystalline SiC hollow spheres are derived at higher temperature. The manuscript is constructed as follows. (1) First of all, macroscopic phase separation of Span 80 in a composite film was investigated. After the microdomains were dissolved from the film, macropores were formed. This provides the experimental base for formation of hollow cavities once the system is processed into droplets. (2) The droplets were fabricated by aerosol-assisted spraying of the sol. During solvent evaporation, the microdomains formed within the drops, which would be templates for hollow cavities after they were removed. Meanwhile, the shell became mesoporous due to the release of small molecules during the cross-linking of phenolic resin at high temperature. (3) Besides structure control, the shell composition could be further transformed at elevated temperature, while the mesoporous and hollow features were retained.

Experimental

Samples synthesis

Materials The chemicals used in this study and their sources are as follows: Phenolic resin was prepared by our group according to literature [21]. Tetraethyl orthosilicate (TEOS), hydrochloric acid (HCl), ethanol, and sorbitan monooleate surfactant (Span 80) were purchased from Beijing Beihua Fine Chemical Co., Ltd (China). Pluronic P123 (M_w=5,800, $EO_{20}PO_{70}EO_{20}$) was from BASF Company (Germany). All the chemicals were used as received without any further purification.

Preparation of a model porous film The porous thin films were prepared similar to literature except the addition of Span 80 [21]. In a typical procedure, 0.6 g of block copolymer P123/Span 80 mixture with different weight ratio was dissolved in 100 g of ethanol under stirring for 1 h at 40 °C until they were completely dissolved. TEOS (0.4 g) and phenolic resin (0.6 g) were added into the solution under stirring for 2 h. The mixture was spread onto a glass plate and stood for 24 h to evaporate ethanol. Cross-linking of phenolic resin and further gelation of silica were achieved by thermal treatment at 100 °C for 24 h in nitrogen. The composite films were calcined at 450 °C in nitrogen to get the porous composite film. The samples were listed in Table 1.

Table 1 Porosity data of some representative materials calculated from the nitrogen adsorption/desorption characterization

Samples[a]	BET surface area ($m^2.g^{-1}$)	Pore volume ($cm^3.g^{-1}$)	Weight ratio of phenolic resin to TEOS	Weight ratio of Span 80 to P123	Treatment temperature and atmosphere
MP-FA-450	537	0.46	3/2	0/1	450, N_2
MP-FB-450	423	0.40	3/2	1/1	450, N_2
MP-SA-180	14	0.02	3/2	1/1	180, N_2
MP-SA-350	375	0.19	3/2	1/1	350, N_2
MP-SA-450	514	0.27	3/2	1/1	450, N_2
MP-SA-550	664	0.54	3/2	1/1	550, N_2
MP-SA-900	937	0.47	3/2	1/1	900, N_2
MP-SA-900-C	1082	0.63	3/2	1/1	900, N_2, HF washing
MP-SA-1450-SiC	598	0.29	3/2	1/1	1,450, Ar
MP-SB-450	465	0.20	3/2	4/1	450, N_2
MP-SC-450	700	0.28	3/2	0/0	450, N_2
MP-SD-450	546	0.42	3/1	1/1	450, N_2

[a] The sample name MP-FX MP-SX indicated the mesoporous films spheres with different composition, respectively. A, B, C, and D denotes changeable phenolic resin content or Span 80 content while the concentration of other components in precursor solution is fixed as recipe 1 (in experiment section) accordingly

Preparation of the hollow spheres The hollow spheres were synthesized by an ultrasonic spraying aerosol-assisted procedure. The precursor solutions were prepared by addition of phenolic resin, TEOS, nonionic surfactant Pluronic P123 and Span 80 into ethanol. Under flowing nitrogen at a volumetric flow rate of 4 L/min, the atomization gas passed through a spiral tube of 6 m long, which was preheated to 200 °C. HCl was gassed into the tube to catalyze sol–gel process of silica and cross-linking of phenolic resin. In a typical experiment, the corresponding weight ratios of the phenolic resin, TEOS, P123, and Span 80 to ethanol were 6, 4, 3, and 3 wt.‰, respectively. The above recipe was denoted as recipe 1. The composite spheres were collected in an aqueous solution, centrifuged, and washed by ethanol. The as-prepared composite spheres were treated at different temperatures, such as 450 °C, 900 °C, and 1,450 °C. Both surfactants were removed by calcination at 450 °C in nitrogen, obtaining the mesoporous hollow spheres of phenolic resin/silica composite. The mesoporous hollow silica spheres were obtained after the composite hollow spheres were calcined at 550 °C in air to selectively remove polymers. The hollow phenolic resin spheres were obtained after the composite hollow spheres were washed with 10 wt.% hydrofluoric acid to selectively remove the silica. The mesoporous carbon/silica and silicon carbide hollow spheres were obtained by further treating the composite spheres at 900 °C in nitrogen and 1,450 °C in argon, respectively. The mesoporous hollow carbon spheres were obtained after the composite carbon/silica hollow spheres were washed with 10 wt.% hydrofluoric acid to remove the silica. All the samples were also listed in Table 1.

Characterization

Transmission electron microscopy (TEM) images were taken with a JEOL 100CX electron microscope with an accelerating voltage of 100 kV. The samples were prepared by dispersing the spheres in ethanol and dropped onto carbon coated copper grids. High-resolution TEM (HR-TEM) characterization was performed on HITACHI H-9000 NAR with an accelerating voltage of 300 kV. Scanning electron microscopy (SEM) images and energy dispersive X-ray (EDX) analysis were taken with a HITACHI S-4300 apparatus operated at an accelerating voltage of 15 kV. The samples were dropped onto the silicon slides, ambient dried, and vacuum sputtered with Pt. Infrared spectra of the samples were recorded on a BRUKER EQUINOX 55 FT-IR spectrometer. The samples were pressed with KBr for measurement. Raman spectra were obtained using a Laser Micro-Raman Spectrometer (Renishaw 2000) with an excitation wavelength of 632.8 nm. X-ray powder diffraction (XRD) data were acquired on a Rigaku D/max-2500 X-ray diffractometer equipped with monochromated Cu Kα radiation (λ= 1.5406 Å). Thermogravimetric analysis (TGA) experiments were performed using the Perkin-Elmer Pyris 1 TGA under nitrogen or air at a heating rate of 10 °C/min. Nitrogen adsorption/desorption isotherms at 77 k for porous spheres were obtained using a Micromeritics ASAP 2020M Surface Area and Porosity Analyzer. The samples were degassed at 300 °C for 11 h. The Brunauer–Emmett–Teller (BET) method was utilized to calculate the specific surface areas. The pore size distributions of the samples were derived from the adsorption branches of the isotherms using the Barrett–Joyner–Halenda method. The total pore volumes, V_p, were estimated from the amount adsorbed at a relative pressure of P/P_0=0.98. The pyrolysis–gas chromatograph–mass spectrometry (Pyr–GC–MS) was carried out by JHP-3S pyrolyzer/GC-17A gas chromatograph/QP-5000 mass spectrometer. The ^{29}Si cross-polarization magic angle spinning nuclear magnetic resonance (CP MAS NMR) spectra were recorded on a Bruker AV 300 solid-NMR spectrometer with the cross-polarization magic angle at 5 kHz and a pulse interval of 5 s. The ^{29}Si chemical shifts were referenced to tetramethylsilane.

Results and discussion

Bimodal porous composite films

Polymers such as polyacrylic acid have been used to obtain macroporous silica by macroscopic phase separation [24, 26, 27], which has been used to synthesize mesoporous hollow silica spheres by aerosol-assisted spraying [25]. However, high molecular polyacrylic acid will result in higher viscosity especially at a high content; it will be difficult to form the aerosol. Besides, the macroscopic phase separation during solvent evaporation will be greatly restricted. Alternatively, we selected small molecular surfactant since rheological performance especially the processability of the studied systems would not be affected. In order to select the surfactant to form macropores, a phenolic resin/silica film was cast from the sol onto a glass plate. When only P123 was used, the film is smooth without macropores (Fig. S1a). When a mixture of Span 80/P123 (1:1 wt/wt) was used, macropores were formed (Fig. S1b). This is resulted from a macroscopic phase separation of Span 80 [28]. As seen from the TEM images of the mesoporous films (Fig. S2a,b), the smooth region of the macroporous film is mesoporous, which means that the mesostructures are less influenced by the addition of

Span 80. The pore size (Fig. S3) is increased from 4.1 to 6.3 nm with the addition of Span 80. Inspired by the above results, we attempt to utilize the phase separation of Span 80 to prepare the composite hollow sphere through aerosol assisted spraying the sols.

Mesoporous composite hollow spheres by aerosol-assisted spraying

The hollow phenolic resin/silica composite spheres with a cavity diameter of 100–200 nm (Fig. 1a) were obtained thereby. After being calcined at 450 °C in nitrogen, the shell became mesoporous (Fig. 1b). The characteristic mesoporous structure was evidenced by the typical type-IV nitrogen sorption isotherm with a hysteresis loop (Fig. 2). As shown in Table 1, the BET specific surface area is 514 $m^2 . g^{-1}$ and the pore volume is 0.27 $cm^3 . g^{-1}$. Complete removal of the surfactants was confirmed by TGA analysis (Fig. S4) and Fourier transform infrared (FTIR) spectra (Fig. S5). Both surfactants were almost completely decomposed in the temperature region 350–480 °C (Fig. S4, traces b and c), the significant weight loss of 30 wt.% of the composite sphere was essentially related to the decomposition of the surfactants (Fig. S4, trace a). FTIR spectra (Fig. S5, traces a–d) shows the characteristic bands around 2,900 and 1,046 cm^{-1} attributed to the C–H and C–O stretching of copolymer P123. A broad band around 3,400 and 1,450 cm^{-1} are assigned to the characteristic stretching mode of phenolic resins and the band at 1,740 cm^{-1} is ascribed to the stretching vibration of Span 80. The decreased intensity of the bands around 2,900 and 1,046 cm^{-1} and the disappearance of the band at 1,740 cm^{-1} are consistent with the surfactant removal shown by TGA.

The calcined phenolic resin/silica composite spheres were further treated with 10 wt.% HF and calcined at 550 °C in air, to selectively remove silica and phenolic resin, respectively. Their spherical shapes (Fig. 1c,d) were well preserved in both cases, revealing that both silica and phenolic resin were continuous in the composite spheres. The bicontinuity of the shell could be achieved within a broad weight ratio of phenolic resin/TEOS ranging from 1/3 to 3/1.

Mechanistic investigation of the hollow cavities and mesopores formation

In order to investigate the formation of hollow cavities, some control experiments were designed. In the absence of Span 80, no hollow spheres were obtained (Fig. S6a). This indicates that the formation of the hollow cavity is closely related with Span 80. The hollow spheres were prepared at different content of Span 80. At a high content level of Span 80 (Span 80/P123 weight ratio above 1:1), the single hollow cavity was predominantly formed, whose size was increased with the increase of Span 80 (Figs. S6b and 1a). Multiple cavities (Fig. S6c) in the hollow spheres were observed at a low content level of Span 80. It can be

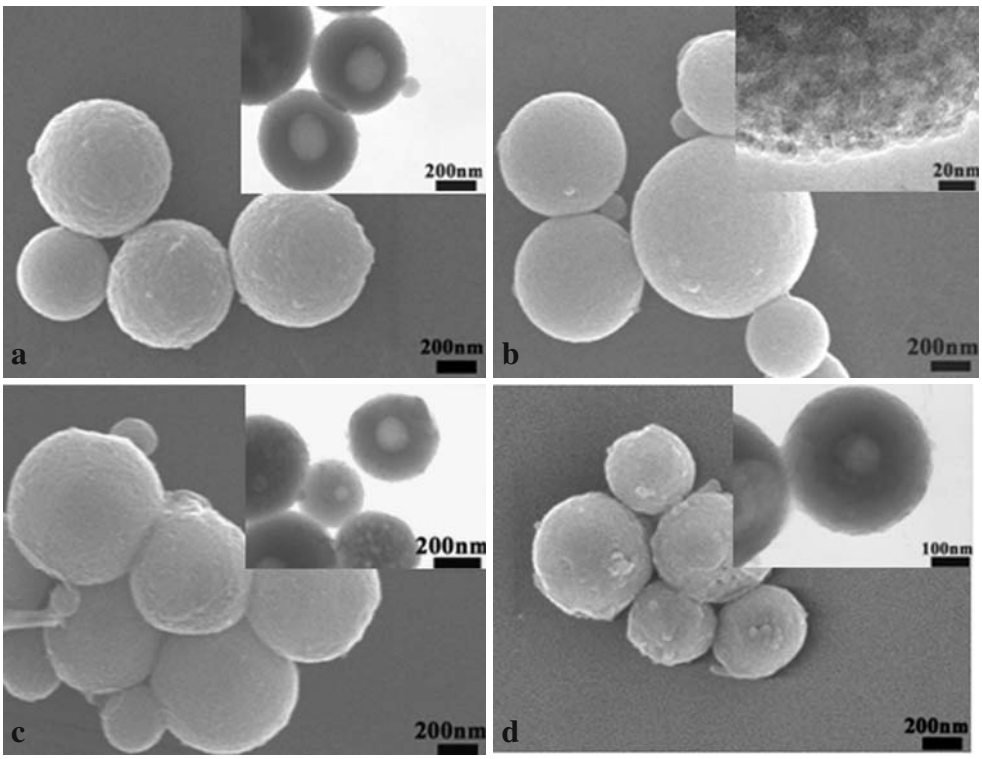

Fig. 1 SEM images of some representative spheres, *inset* the TEM images: **a** the as-prepared spheres MP-SA, **b** the same composite spheres as Fig. 1a but after removing the surfactants, **c** the phenolic resin hollow spheres, and **d** the silica hollow spheres derived from the composite spheres as shown in Fig. 1b after removal of the silica by 10 wt.% HF and phenolic resin by calcination at 550 °C in air, respectively

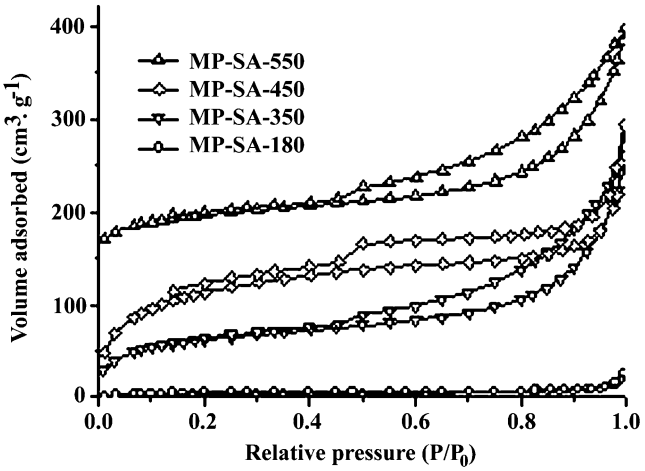

Fig. 2 Nitrogen adsorption/desorption isotherms of the spheres MP-SA after being calcined under different temperature

explained by an easier and more complete phase separation of Span 80 from less viscous system prior to the shell solidification when Span 80 content is high. In contrast, at a low content, the phase separation is restricted by the increased viscoelastic system, thus, forming multiple domains thereby. This finding is similar with the phase separation of polyacrylic acid [29]. Therefore, both size and number of the hollow cavity can be controlled by changing Span 80 content.

It should be mentioned that the acidic HCl gas played an important role in the shell solidification and formation of the hollow composite spheres. When HCl vapor was absent in the carrying gas, the shell became disintegrated (Fig. S6d), and hollow cavities were exposed to their surroundings. The exterior shell structure of the spheres could be controlled by changing the introduction level of HCl vapor.

It is another important issue to understand how the mesopores are formed besides the hollow cavities. After the as-prepared composite spheres were heated at 180 °C in nitrogen for 4 h to further cross-link the phenolic resin, they were treated with ethanol to remove the surfactants. The complete extraction of the surfactants was confirmed by FTIR results (Fig. S7). The BET specific surface area is 14 $m^2. g^{-1}$ and the pore volume is 0.02 $cm^3. g^{-1}$ (Fig. 2), indicating that the spheres have no interconnected mesopores. This unexpected result indicates that the surfactant P123 did not self-assemble into supramolecular templates, thus, forming mesopores. However, the mesopore appeared after the composite hollow spheres were further treated at 450 °C in nitrogen. This is attributed to the release of small molecules from the phenolic resin moiety of the composite spheres, which was confirmed by Pyr–GC–MS spectra at a representative temperature 445 °C under nitrogen (Fig. S8a). As a comparison, small molecules were also detected around the same elution time from pure phenolic resin (Fig. S8b). Furthermore, ^{29}Si magic angle spinning NMR spectrum (Fig. S9) of silica in the composite spheres showed that hydrolysis of TEOS-forming silica was complete without any organic pendant groups [30]. It has been excluded that the formation of the mesopores may be related with incomplete hydrolysis of TEOS-forming silica. Calcination of the composite spheres at a temperature ranging 350–550 °C would result in mesopores (Fig. 2), the specific surface area, and pore volume (Table 1) increased at an elevated temperature. Higher specific surface area and larger pore volume were gained by increasing phenolic resin content (e.g., sample MP-SD-450; Table 1). The nitrogen adsorption/desorption isotherms (Fig. S10) of the MP-SD-450 spheres exhibit a rather broad capillary condensation step, indicating the existence of relatively disordered mesopores. In the absence of both surfactants, solid composite spheres MP-SC instead of hollow ones were prepared (Fig. S6e). After they were calcined at 450 °C, a high BET specific surface area of 700 $m^2. g^{-1}$ and a pore volume of 0.28 $cm^3. g^{-1}$ was detected (Fig. S10; Table 1). Therefore, the mesopores are essentially originated from small molecules release during cross-linking of the phenolic resin [31]. Since the mesopores are formed by release of small molecules from phenolic resins at high temperature, some key parameters of the materials such as the average pore size, specific surface area, and the pore volume can, thus, be controlled by either changing the content of the phenolic resin or the calcination temperature (Table S1).

Composition transformation

Since phenolic resin is a good precursor for carbon, it is interesting to derive carbon-based hollow spheres starting from phenolic resin/silica composite spheres. After the composite spheres were treated at 900 °C in nitrogen, the carbon/silica composite hollow spheres were obtained. The spherical contour was well preserved with the mesoporous shell retained (Fig. 3a). The mesopore size distribution became broader (Fig. 4). The obtained mesoporous carbon/silica sphere has a BET specific surface area of 937 $m^2. g^{-1}$ and a pore volume of 0.47 $cm^3. g^{-1}$. Raman spectra (Fig. S11) and XRD pattern (Fig. 5, trace a) indicate that the carbon in the composite sphere is amorphous. The corresponding carbon spheres and silica spheres were obtained by removing the silica component by HF or carbon by calcination in air, respectively. Complete removal of the silica was confirmed by EDX spectroscopy (Fig. S12). The obtained carbon sphere was mesoporous with a higher BET specific surface area of 1,082 $m^2. g^{-1}$ and a pore volume of 0.63 $cm^3. g^{-1}$ (Fig. 4). As shown in Fig. 3b–d, the spherical shape of the corresponding carbon and silica spheres was preserved

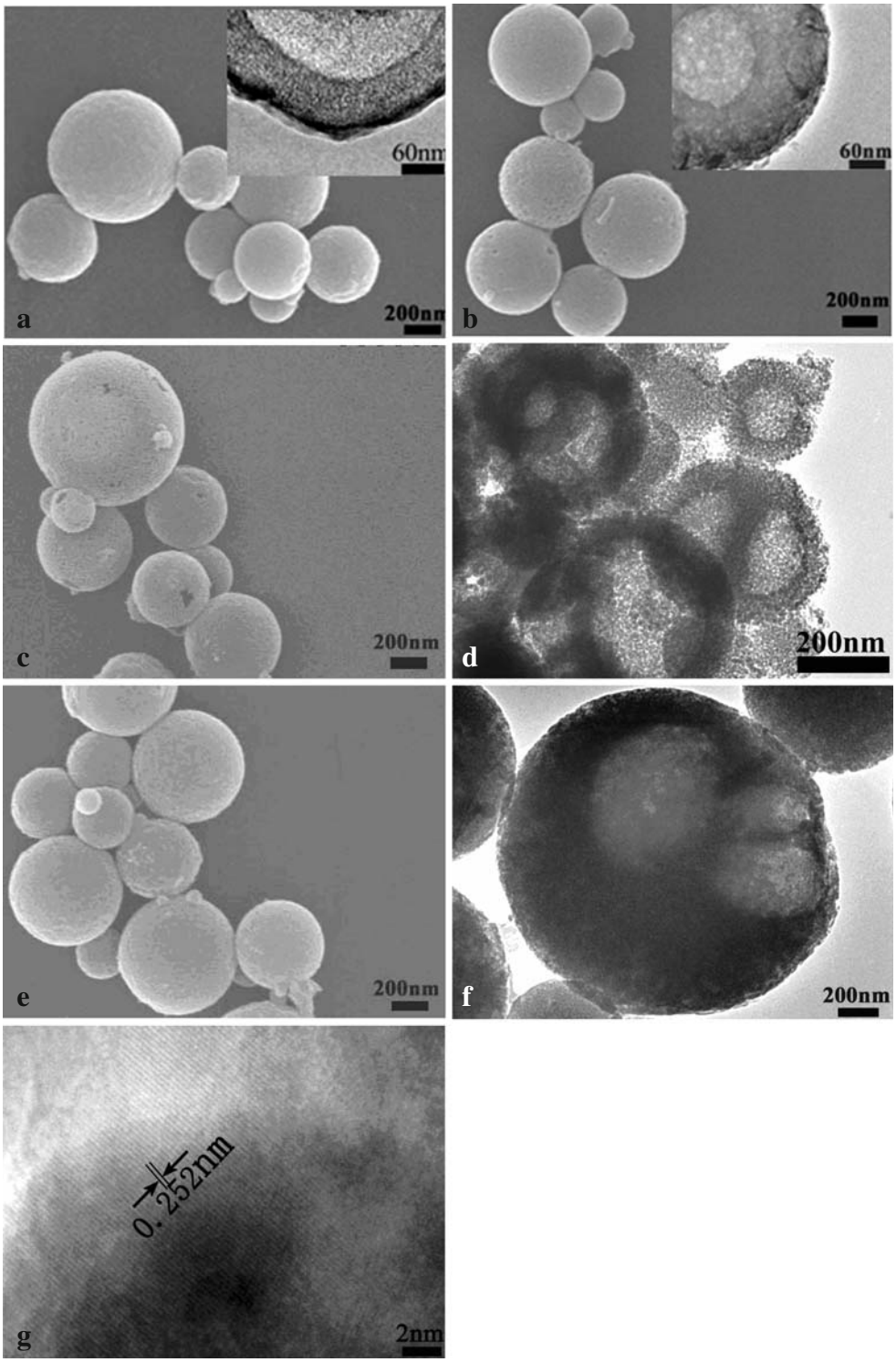

Fig. 3 Morphology of some representative spheres derived from the spheres MP-SA in Fig. 1a: **a** SEM image of carbon/silica composite spheres *inset* HR-TEM image, **b** SEM image of hollow carbon spheres derived from the spheres in Fig. 3a *inset* HR-TEM image, **c** SEM image of hollow silica spheres derived from the spheres in Fig. 3a, **d** TEM image of the hollow silica spheres derived from the spheres in Fig. 3a, and **e**–**g** SEM, TEM, and HR-TEM images of the hollow silicon carbide spheres

with the mesoporous shell retained. This fact further indicates that the carbon/silica composite spheres are bicontinuous. After the silica/carbon composite hollow spheres were further treated at a higher temperature of 1,450 °C for 4 h under argon, dark green SiC hollow spheres were obtained (Fig. 3e,f). Shell of the silicon carbide spheres was disordered mesoporous (Fig. 4). The sphere has a BET specific surface area of 598 $m^2 . g^{-1}$ and a pore volume of 0.29 $cm^3 . g^{-1}$. The appearance of the characteristic band at 870 cm^{-1} is assigned to the Si–C vibration (Fig. S13), indicating the generation of SiC. XRD (Fig. 5, trace c) result and the HR-TEM image (Fig. 3g) show that the shell SiC is in the form of β-SiC phase with a lattice parameter 0.252 nm, consistent with a pure β-SiC

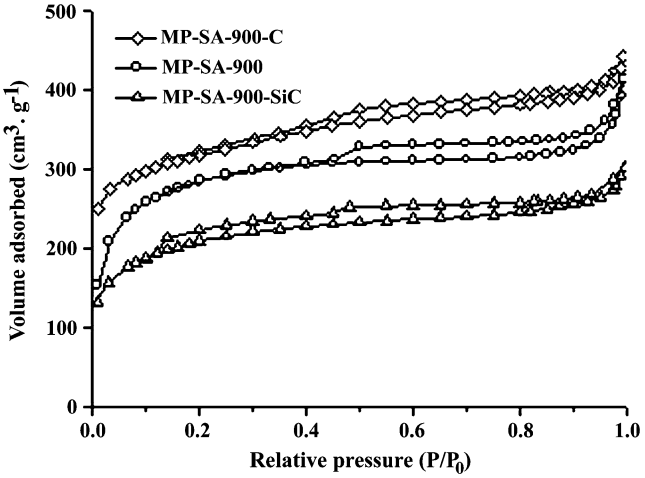

Fig. 4 Nitrogen adsorption/desorption isotherms of MP-SA-900 and the derivatives

[32]. The β-SiC content can be controlled by changing treatment temperature. At a decreased treatment temperature from 1,450 °C to 1,300 °C, the β-SiC phase content became lower (Fig. 5, trace b).

Thermal stability of carbon materials especially in air is crucial in catalysis. Pure carbon (Fig. 6a) spheres prepared by carbonization of phenolic resins lost their weight progressively with temperature. In comparison, no weight loss was found for the carbon/silica composite spheres until 450 °C (Fig. 6b). For the silicon carbide spheres, no significant weight loss was detected (Fig. 6c) even at 800 °C in air. Therefore, compared to the pure carbon spheres, the thermal oxidative stability of the carbon-based composite spheres is enhanced greatly.

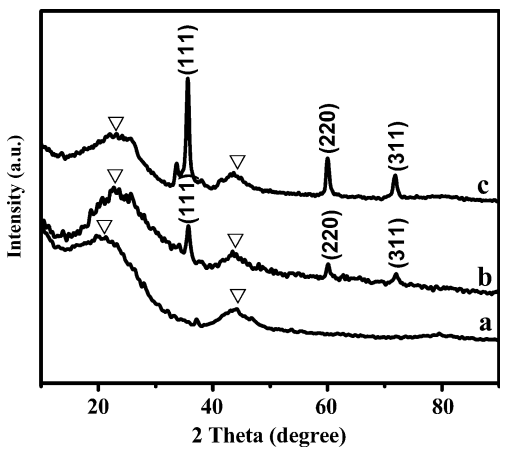

Fig. 5 XRD patterns of some representative spheres derived from the spheres as shown in Fig. 1a: **a** carbon/silica spheres, **b** the silicon carbide hollow spheres after calcination at 1,300 °C in argon, **c** the silicon carbide hollow spheres after calcinations at 1,450 °C in argon. *unfilled inverted triangle* The amorphous carbon

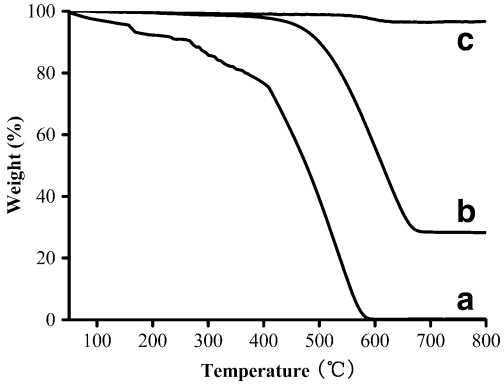

Fig. 6 TGA traces of different samples recorded in air: **a** the pure carbon, **b** the carbon/silica spheres, and **c** the hollow silicon carbide spheres derived from the spheres MP-SA in Fig. 1a

Conclusions

The phenolic resin/silica composite hollow spheres have been synthesized by ultrasonic spraying in combination with the macroscopic phase separation of small molecular surfactant Span 80 during solvent evaporation. Size and number of the hollow cavities can be tuned by adjusting Span 80 content. Within the shell, phenolic resin and silica are both continuous. The shell composition can be transformed into carbon/silica and SiC at high temperature, whilst the shell becomes mesoporous after small molecules are released. Thermal stability in air of the carbon-based composite mesoporous hollow spheres has been greatly improved by the introduction of silica. This will be promising to provide supporting carbon catalysts with enhanced thermal oxidative stability for fuel cells.

Supporting information available

The pore size dependence on the phenolic resin weight ratio and temperature; Some characterization on the mesoporous film including SEM, TEM, nitrogen adsorption measurement; TGA traces and FTIR spectra of some samples; The Pyr–GC–MS chromatograph data and ^{29} Si CP MAS NMR spectra of the composite spheres MP-SA after cross-linking at 180 °C and remove the surfactants; Nitrogen adsorption of some control samples; SEM and TEM images of some control samples; Raman spectra of the composite carbon/silica spheres; SEM-based energy-dispersive X-ray spectroscopy spectra of the carbon spheres; FTIR spectra of the corresponding carbon/silica and silicon carbide spheres.

Acknowledgment We thank financial support by the National Natural Science Foundation of China (50573083, 50521302, 50733004, and 20720102041), Chinese Academy of Sciences and the China Ministry of Science and Technology (2006CB605300 and 2003CB615600) is acknowledged.

References

1. Anderson M, Holmes WS, Hanif MN, Cundy CS (2000) Angew Chem Int Ed 39:2707–2710
2. Smått J, Schunk S, Lindén M (2003) Chem Mater 15:2354–2361
3. Zhong Z, Yin Y, Gates B, Xia YN (2000) Adv Mater 12:206–209
4. Caruso F (2000) Chem Eur J 6:413–419
5. Wilcox DL, Bernat MT, Kelleman D, Cochran JK (1994) Hollow and solid spheres and microspheres: science and technology associated with their fabrication and application, vol 372. Materials Research Society Proceedings, Pittsburgh
6. Vallet-Regi M, Rámila A, del Real RP, Pérez-Pariente J (2001) Chem Mater 3:308–311
7. Fisher KA, Huddersman KD, Taylor MJ (2003) Chem Eur J 9:5873–5878
8. Zhu YF, Shi JL, Li YS, Chen HR, Shen WH, Dong XP (2005) Micropor Mesopor Mater 85:75–81
9. Kresge CT, Leonowicz ME, Roth WJ, Vartuli JC, Beck JS (1992) Nature 359:710–712
10. Beck JS, Vartuli JC, Roth WJ, Leonowicz ME, Kresge CT, Schmitt KD, Chu CT-W, Olson DH, Sheppard EW, McCullen SB, Higgins JB, Schlenker JL (1992) J Am Chem Soc 114:10834–10843
11. Firouzi A, Atef F, Oertli AG, Stucky GD, Chmelka BF (1997) J Am Chem Soc 119:3596–3610
12. Zhao DY, Feng J, Huo Q, Melosh NG, Frederickson H, Chmelka BF, Stucky GD (1998) Science 279:548–552
13. Li YS, Shi JL, Hua ZL, Chen HR, Ruan ML, Yan DS (2003) Nano Lett 3:609–612
14. Choi M, Kleitz F, Liu DN, Lee HY, Ahn W, Ryoo R (2005) J Am Chem Soc 127:1924–1932
15. Asefa T, MacLachlan MJ, Coombs N, Ozin GA (1999) Nature 402:867–871
16. Pang J, John VT, Loy DA, Yang ZZ, Lu YF (2005) Adv Mater 17:704—707
17. Giunta PR, van de Burgt LJ, Stiegman AE (2005) Chem Mater 17:1234–1240
18. Ryoo R, Joo SH, Jun S (1999) J Phys Chem B 103:7743–7746
19. Jun S, Joo SH, Ryoo R, Kruk M, Jaroniec M, Liu Z, Ohsuna T, Terasaki O (2000) J Am Chem Soc 122:10712–10713
20. Liu R, Shi Y, Wan Y, Meng Y, Zhang F, Gu D, Chen ZX, Tu B, Zhao DY (2006) J Am Chem Soc 128:11652–11662
21. Meng Y, Gu D, Zhang FQ, Shi YF, Yang HF, Li Z, Yu CZ, Tu B, Zhao DY (2005) Angew Chem Int Ed 44:7053–7059
22. Hu QY, Kou R, Pang J, Ward TL, Cai M, Yang ZZ, Lu YF, Tang J (2007) Chem Commun 6:601–603
23. Yan Y, Zhang FQ, Meng Y, Tu B, Zhao DY (2007) Chem Commun 27:2867–2869
24. Nishino H, Takahashi H, Sato S, Sodesawa T (2004) J Non-Cryst Solids 333:284–290
25. Rathod SB, Ward TL (2007) J Mater Chem 17:2329–2335
26. Nakanishi K, Takahashi R, Nagakane T, Kitayama K, Koheiya N, Shikata H, Soga N (2000) J Sol–Gel Sci Technol 17:191–210
27. Nakanishi K, Soga N (1992) J Non-Cryst Solids 139:1–13
28. Vogelaar L, Lammertink RGH, Barsema JN, Nijdam W, Bolhuis-Versteeg LAM, van Rijn CJM, Wessling M (2005) Small 1: 645–655
29. Nakanishi K, Soga N (1992) J Non-Cryst Solids 139:14–24
30. Kaji H, Nakanishi K, Soga N (1995) J Non-Cryst Solids 181: 16–26
31. Yang M, Ma J, Ding SJ, Meng ZK, Liu JG, Zhao T, Mao LQ, Shi Y, Jin XG, Lu YF, Yang ZZ (2006) Macromol Chem Phys 207:1633–1639
32. Yang ZX, Xia YD, Mokaya R (2004) Chem Mater 16:3877–3884